frontiers | Frontiers in Cellular and Infection Microbiology

ORIGINAL RESEARCH
published: 23 May 2022
doi: 10.3389/fcimb.2022.849017

Characterization of the Interaction Between SARS-CoV-2 Membrane Protein (M) and Proliferating Cell Nuclear Antigen (PCNA) as a Potential Therapeutic Target

*Érika Pereira Zambalde[1], Isadora Carolina Betim Pavan[2], Mariana Camargo Silva Mancini[1], Matheus Brandemarte Severino[1], Orlando Bonito Scudero[3], Ana Paula Morelli[1], Mariene Ribeiro Amorim[4], Karina Bispo-dos-Santos[4], Mariana Marcela Góis[1], Daniel A. Toledo-Teixeira[4], Pierina Lorencini Parise[4], Thais Mauad[5], Marisa Dolhnikoff[5], Paulo Hilário Nascimento Saldiva[5], Henrique Marques-Souza[6], José Luiz Proenca-Modena[4,7,8], Armando Morais Ventura[3] and Fernando Moreira Simabuco[1]**

[1] Multidisciplinary Laboratory of Food and Health, School of Applied Sciences, University of Campinas (Unicamp), Limeira, Brazil, [2] Laboratory of Signaling Mechanisms, School of Pharmaceutical Sciences, University of Campinas, (Unicamp), Campinas, Brazil, [3] Department of Microbiology, Institute of Biomedical Sciences, University of São Paulo (USP), São Paulo, Brazil, [4] Laboratory of Emerging Viruses (LEVE), Department of Genetics, Evolution, Microbiology and Immunology, Institute of Biology, University of Campinas (Unicamp), Campinas, SP, Brazil, [5] São Paulo University Medical School, Department of Pathology, University of São Paulo (USP), São Paulo, Brazil, [6] Institute of Biology, University of Campinas (Unicamp), Campinas, SP, Brazil, [7] Experimental Medicine Research Cluster, University of Campinas (Unicamp), Campinas, Brazil, [8] Hub of Global Health (HGH), University of Campinas (Unicamp), Campinas, Brazil

SARS-CoV-2 is an emerging virus from the Coronaviridae family and is responsible for the ongoing COVID-19 pandemic. In this work, we explored the previously reported SARS-CoV-2 structural membrane protein (M) interaction with human Proliferating Cell Nuclear Antigen (PCNA). The M protein is responsible for maintaining virion shape, and PCNA is a marker of DNA damage which is essential for DNA replication and repair. We validated the M-PCNA interaction through immunoprecipitation, immunofluorescence co-localization, and PLA (Proximity Ligation Assay). In cells infected with SARS-CoV-2 or transfected with M protein, using immunofluorescence and cell fractioning, we documented a reallocation of PCNA from the nucleus to the cytoplasm and the increase of PCNA and γH2AX (another DNA damage marker) expression. We also observed an increase in PCNA and γH2AX expression in the lung of a COVID-19 patient by immunohistochemistry. In addition, the inhibition of PCNA translocation by PCNA I1 and Verdinexor led to a reduction of plaque formation in an *in vitro* assay. We, therefore, propose that the transport of PCNA to the cytoplasm and its association with M could be a virus strategy to manipulate cell functions and may be considered a target for COVID-19 therapy.

Keywords: SARS-CoV-2, PCNA, M protein, viral-host interaction, DNA damage

OPEN ACCESS

Edited by:
Vikas Sood,
Jamia Hamdard University, India

Reviewed by:
Henri Gruffat,
Institut National de la Santé et de la Recherche Médicale (INSERM), France
Manish SHarma,
Emory University, United States

***Correspondence:**
Fernando Moreira Simabuco
simabuco@gmail.com
orcid.org/0000-0002-1672-9686

Specialty section:
This article was submitted to Virus and Host, a section of the journal Frontiers in Cellular and Infection Microbiology

Received: *05 January 2022*
Accepted: *25 April 2022*
Published: *23 May 2022*

Citation:
Zambalde ÉP, Pavan ICB, Mancini MCS, Severino MB, Scudero OB, Morelli AP, Amorim MR, Bispo-dos-Santos K, Góis MM, Toledo-Teixeira DA, Parise PL, Mauad T, Dolhnikoff M, Saldiva PHN, Marques-Souza H, Proenca-Modena JL, Ventura AM and Simabuco FM (2022) Characterization of the Interaction Between SARS-CoV-2 Membrane Protein (M) and Proliferating Cell Nuclear Antigen (PCNA) as a Potential Therapeutic Target. Front. Cell. Infect. Microbiol. 12:849017. doi: 10.3389/fcimb.2022.849017

INTRODUCTION

The COVID-19 was claimed as a global public health emergency by the World Health Organization (WHO). By April 07th, 2022, more than 495 million cases were confirmed, with more than 6.17 million deaths worldwide (WHO- World Health Organization, 2020). COVID-19 is caused by SARS-CoV-2, an emerging virus from the *Coronaviridae* family of positive single-stranded RNA genome that encodes over 28 proteins, including 16 non-structural proteins (NSP1- NSP16), four structural proteins (spike, membrane, envelope, and nucleocapsid), and eight auxiliary proteins (ORF3a, ORF3b, ORF6, ORF7a, ORF7b, ORF8, ORF9b, and ORF14) (Gordon et al., 2020; Sanche et al., 2020; Wu et al., 2020). The four main structural proteins of the virion are responsible for: cell receptor recognition - spike (S); viral RNA packaging - nucleocapsid (N); and virus assembly - envelope (E) and membrane (M) proteins (Thiel et al., 2003; Chen et al., 2020; Klein et al., 2020).

Nearly two years after the start of the pandemic, no treatment has yet been successful, and the infection mechanisms are still an open question (Song et al., 2020). Many studies have been dedicated to understanding the interactome of SARS-CoV-2 with infected cells (Bouhaddou et al., 2020; Gordon et al., 2020; Li et al., 2021; Stukalov et al., 2021). The interaction between the structural protein M of SARS-CoV-2 and the human protein Proliferating Cell Nuclear Antigen (PCNA) was described with a Significance Analysis of INTeractome (SAINT) score of 1.0 (Gordon et al., 2020), indicating a high probability of interaction. In addition, Stukalov et al. (2021) showed increased ubiquitination in specific regions (K13, K14, K77, K80, K248, and K254) of PCNA in cells infected with SARS-CoV-2 when compared to a control group.

M is the most abundant structural protein in the SARS-CoV-2 particle and is highly expressed (Neuman et al., 2011; Wyler et al., 2020; Alharbi and Alrefaei, 2021). M is responsible for giving and maintaining the virion's shape (Hasan and Hossain, 2020), is a three-pass membrane protein with three transmembrane domains and co-localizes with the endoplasmic reticulum (ER), Golgi apparatus, and mitochondrial markers (Hasan and Hossain, 2020; Zhang et al., 2020; Zheng et al., 2020). In addition, the M protein can interact with different coronavirus (CoVs) proteins: the N protein, which helps in viral genome packing (Hurst et al., 2005; Kuo et al., 2016; Lu et al., 2021), and the S protein, for its retention in the ER-Golgi intermediate compartment and its integration into new virions (Opstelten et al., 1995).

It was demonstrated that, in some CoVs, the M protein is highly immunogenic and induces specific T-cell responses after infection (Li et al., 2008). In SARS-CoV-2 infection, M is also targeted by the immune response and plays a critical role in virus-specific B-cell response due to its ability to induce the production of efficient neutralizing antibodies in COVID-19 patients (Pang et al., 2004; Alharbi and Alrefaei, 2021). During SARS-CoV-2 infection, the M protein can directly bind to MAVS (Mitochondrial Antiviral Signaling Protein) to inhibit the innate immune response (Fu et al., 2021). More specifically, the SARS-CoV-2 M protein antagonizes type I and III interferon (IFN) production by targeting RIG-I/MDA-5 signaling and preventing the multiprotein complex formation of RIG-I, MAVS, TRAF3, and TBK1. This multiprotein complex blocks the activation of IRF3-induced anti-viral immune suppression, facilitating virus replication (Zheng et al., 2020; Fu et al., 2021). Although the M protein binding to MAVS mechanism has been described, other authors suggest that M is mainly involved in ATP biosynthesis and metabolic processes (Bojkova et al., 2020; Li et al., 2021), indicating that it has different functions.

The PCNA is a 36 kDa protein, well-conserved in all eukaryotic species, from yeast to humans (Strzalka and Ziemienowicz, 2011). This protein controls essential cellular processes such as DNA replication and damage repair, transcription, chromosome segregation, and cell-cycle progression (Tsurimoto, 1998; Paunesku et al., 2001; Maga and Hübscher, 2003; Naryzhny et al., 2005; Moldovan et al., 2006; Strzalka and Ziemienowicz, 2011). It has been dubbed the "maestro of the replication fork" (Moldovan et al., 2007). PCNA, as a homotrimer, encircles duplex DNA, forming a ring-shaped clamp (Warbrick, 1998). The PCNA is a scaffolding protein that interacts with several other proteins, mainly involved in DNA replication and repair (Maga and Hübscher, 2003). In most cell types, PCNA is exclusively nuclear, but studies demonstrated that it could go to the cytoplasm. In cancer cells, cytoplasmic PCNA was described as a regulator of the cell metabolism binding to enzymes involved in the glycolysis pathway, regulation of the energy-generating system in mitochondria, cytoskeleton integrity, and other cellular signaling pathways through binding to cytoplasmic and membrane proteins (Naryzhny and Lee, 2010). PCNA is cytosolic in mature neutrophils and acts in immune response, including to virus infection (Witko-Sarsat et al., 2010; Bouayad et al., 2012; Olaisen et al., 2015; Ohayon et al., 2019).

Although many studies indicate the PCNA role in DNA virus infection, its association with RNA viruses is poorly understood. To our knowledge, the only study that observed a function of PCNA in an RNA virus was with the Bamboo Mosaic virus (BaMV), a common virus in plants. In this study, the authors demonstrated that PCNA goes to the cytoplasm and directly binds to the BaMV replication complex, downregulating the replication efficiency of the virus (Lee et al., 2019).

In this study, we validated the M-PCNA interaction and demonstrated that the M protein facilitates the transport of PCNA from the nucleus to the cytoplasm. M expression and SARS-CoV-2 infection were associated with increased phosphorylation of H2AX and an increased PCNA expression. Drugs that block PCNA translocation from nucleus to cytoplasm inhibited virus replication. This indicates a new mechanism in SARS-CoV-2 replication and a potential target for therapy.

MATERIALS AND METHODS

Cell Culture

The VeroE6 (African green monkey, *Cercopithicus aethiops*, kidney) and HEK293T (Human embryonic kidney) cell lines

were cultivated in Dulbecco's modified Eagle (DMEM) (Thermo Scientific #12100-046) medium, supplemented with 10% fetal bovine serum (FBS # 12657029) and 1% penicillin/streptomycin (Gibco #15140-122). Cells were maintained at 37°C in a humidified atmosphere containing 5% carbon dioxide.

Viral Infection

An aliquot of SARS-CoV-2 SP02.2020 (GenBank accession number MT126808) isolate was kindly donated by Dr. Edison Luiz Durigon (Institute of Biomedical Sciences, University of São Paulo). Vero E6 cells were used for virus propagation in the Biosafety Level 3 Laboratory (BSL-3) of the Laboratory of Emerging Viruses (Institute of Biology, State University of Campinas). Viral infections were performed in Vero cells seeded in 24-well plates (5×10^5 cells/well) for the experiments with treatments and immunofluorescence assays, and six-well plates (1×10^6 cells/well) for Western blots. A multiplicity of infection (MOI) of 0.3 was used for all experiments.

Cloning

To do the FLAG-tagged protein expression, a modified pcDNA 3.1 (+) (Thermo Fisher Scientific) was generated by cloning the FLAG peptide coding sequence upstream of the multiple cloning sites, using the *Nhe*I and *Bam*HI restriction sites, and generating the pcDNA-FLAG vector (Oliveira et al., 2013). The full-length of M, N, and E genes were codon-optimized, synthesized (Geneart -Thermo Fisher Scientific), and cloned into pcDNA-FLAG, generating plasmid pFLAG-M, pFLAG-N, and pFLAG-E. The pFLAG-green fluorescent protein (GFP) (Amaral et al., 2016) was used as the control plasmid for the expression of a non-related protein in the immunoprecipitation assays.

Transfection

VeroE6 and HEK293T cells were seeded for 24 hours before transfection. Transfection was performed with Lipofectamine (Thermo Scientific - #20071882) and PLUS reagents (Thermo Scientific - #15338100). The protocol of plasmids' transfection is described by (Amaral et al., 2016). For immunofluorescence, the cells were seeded and transfected in 24-well plates; for western blotting in 6-well plates; and for immunoprecipitation in 100 mm plates.

Immunoprecipitation

For anti-FLAG immunoprecipitation, HEK293T cells cultivated in 100 mm diameter dishes expressing the FLAG-tagged GFP, E, M, and N proteins were washed twice with PBS and harvested by pipetting up and down in PBS after 48 hours. Cells were resuspended in 500 µL of lysis buffer (50 mM Tris-HCl, pH 7.4, 150 mM NaCl, 1 mM EDTA, 1% Triton X-100) containing protease inhibitor cocktail (Roche). Protein lysates were incubated and shaken on ice for 15 min and centrifuged at 12,000 × g for 10 min at 4°C. Supernatants were collected and protein quantification was performed using a BCA protein assay kit (Thermo Scientific). A total of 2,000 µg of protein extract was used to perform the immunoprecipitation, so the samples were diluted with lysis buffer without inhibitors and incubated overnight at 4°C with 30 µL of anti-FLAG agarose-coupled beads (#A2220, Sigma-Aldrich) under mild agitation. Subsequently, the beads were washed five times with 600 µL of ice-cold TBS (50 mM Tris-HCl, pH 7.5, 150 mM NaCl) and eluted with 300 ng/L of FLAG peptide (#F4799, Sigma-Aldrich) for four hours under moderate agitation (Pavan et al., 2016). Supernatants were collected and stored at -20°C for immunoblotting analysis.

For reverse immunoprecipitation, in HEK293T cells, the same protocol of protein lysis and quantification were performed. A total of 300 µg of protein extract was used to perform the immunoprecipitation. The samples were diluted with lysis buffer without inhibitors and incubated overnight at 4°C with anti-PCNA antibody (1:500, #2586, Cell Signaling) under mild agitation. Subsequently, 30 µL of protein A/G Agarose (#20421, Thermo Scientific) was added to each sample, followed by mild agitation for two hours. Samples were washed five times with a wash buffer (25 mM Tris-HCl, pH 7.5, 150 mM NaCl) and the elution was performed with Laemmli Buffer with SDS 1×. Supernatants were collected and stored at -20°C for immunoblotting analysis.

Immunofluorescence

Sterilized glass coverslips were treated with 6M HCL (Synth) and placed in each well on 24-well plates. Vero E6 cells were seeded at a density of 1×10^5 cells in DMEM with 10% FBS. After the experimental procedures, the wells were washed 1× with PBS, permeabilized with ice-cold methanol 100% for 10 minutes, or fixed with paraformaldehyde 4% (PFA – Sigma Aldrich 158127) for 15 minutes. The cells were then permeabilized with PBS-Tween-20 0.1% (PBS-T - Sigma Aldrich P1379) for 10 minutes, blocked with 1% BSA-Tween-20 0.3% for 30 minutes, and incubated overnight with a solution containing the primary antibody in (1:200) 1% BSA-Tween-20 0.3% at 4°C. After a washing step with PBS (three times for 10 minutes each), a solution containing the secondary antibody (1:250) and PBS-Tween20 0.1% was added to each well for one hour in a dark chamber. The wells were then washed three times with PBS (for 10 minutes each), a solution containing Hoechst (Sigma Aldrich – 861405 - 1:1,000) was added for 10 minutes, followed by three times washing with PBS (for 10 minutes each), the glass coverslips were removed from the wells with the aid of tweezers and added to glass slides with 5 µL of Glycerol (Sigma Aldrich G5516). The primary antibodies used were: PCNA (Cell Signaling #2586), N (Invitrogen #MA5-35943), FLAG (Sigma # F3165). The secondary antibodies used were: Alexa-Fluor-594 Goat anti-Rabbit (Jackson ImmunoResearch #711-585-152), Alexa-Fluor-488 Goat Anti-Mouse (Jackson ImmunoResearch #705-545-003). To quantify the signal on immunofluorescences we used the ImageJ software to transform the images in 8 bit (grayscale), and check-in Set Measurements the options: Area and Integrated density; select an ROI of nuclei area (Hoechst staining) to determinate the fluorescence signal on nuclei; the cytoplasmatic fluorescence signal was obtained by a total cell - nuclei area ROI. Besides that, we computed the signal of the background (region without

cells). Finally, the Corrected Cell Total Fluorescence (CTCF) was calculated by multiplication of the integrated density of gray of nuclei or cytoplasm by their respective areas and subtracting the background signal.

Subcellular Fractioning

Vero E6 cells were seeded at 8×10^6 in a P100 plate and transfected with pFLAG-GFP or pFLAG-M. After 48 hours, the subcellular fractionation was finalized (Baldwin, 1996). Briefly, the cytoplasmic fraction was first isolated from the nuclear solution using a cytoplasmic buffer (10 mM HEPES; 60 mM KCl; 1 mM EDTA; 0.075% NP-40; 1 mM DTT; protease inhibitor 1×) (pH=7.6) and centrifuged in 1,400×g for 30 minutes. The cytoplasmic supernatants were collected into a new tube. The nuclear pellet was washed with cytoplasmic buffer without NP-40 two times followed by a five-minute centrifugation at 1,000×g. The final pellet was resuspended with nuclear buffer (20 mM TrisCl; 420 mM NaCl; 1.5 mM $MgCl_2$; 0.2 mM EDTA; 25% glycerol; protease inhibitor 1×) (pH=8.0) and incubated on ice for 10 minutes, and vortexed periodically. Finally, the cytoplasmic and nuclear solutions were centrifuged at 12,000×g for 10 minutes and the supernatants were collected into new tubes. The quantification was performed by BCA.

Proximity Ligation Assay (PLA)

For PLA protocol, Vero E6 cells were grown on chambered slides at a confluency of 70% and transfected with pFLAG-M. After 24 hours, cells were fixed with ice-cold methanol for 15 min and permeabilized with 0.1% TritonX-100 in PBS. The next steps faithfully followed the manufacturer's specifications (Duolink® *In Situ* – Sigma-Aldrich). Briefly, cells were blocked and stained with primary antibodies (anti-FLAG 1:400 - Sigma F7425 and anti-PCNA 1:400 – Sta Cruz sc-56) and PLA probes (anti-mouse MINUS - DUO92004 and anti-rabbit PLUS - DUO92002). Then, cells were incubated with Ligase for 30 minutes (37°C) and Polymerase for signal amplification for 100 minutes (37°C) (Duolink® *In Situ* Orange - DUO92102). For negative controls, cells were stained, missing one of the primary antibodies, or both. After all PLA protocol steps, cells were stained with anti-FLAG 1:400 and anti-rabbit Alexa Fluor 488 1:1,000 (Invitrogen - A-11008) to identify transfected cells. Nuclei were stained with DAPI. After the respective washes, slides were mounted with Fluoromount-G (Invitrogen). The contrast was evenly enhanced in all presented images for better visualization of PLA dots.

Confocal Microscopy

For co-localization analysis, images were taken with a Zeiss LSM 780 NLO confocal microscope coupled to a HeNe (543 nm), an Argon (488 nm) and a Diode (405 nm) lasers (Core Facility for Scientific Research – University of Sao Paulo (CEFAP-USP)). Images were acquired with an objective α Plan-Apochromat 100x/NA 1.46 in oil immersion. Fluorescent signal was detected on a 32 channel GaAsP QUASAR detector with the following parameters: Alexa Fluor 594 (578 – 692 nm), Alexa Fluor 488 (491 – 587 nm), DAPI (412 – 491 nm). Pinhole was set to 1 airy unit, and z-stacks were taken with intervals of 340 nm. Presented images show a single representative z-stack. Overlap in signal between different channels was measured with Plot Profile plugin on ImageJ. Images were contrast-enhanced for better visualization.

Western Blotting

The proteins were collected from Vero E6 and HEK293 cells using a cell lysis buffer (50 mM Tris-Cl pH 7.5; 150 mM NaCl, 1 mM EDTA, 1% Triton x-100, and protease and phosphatase inhibitor cocktail). To obtain the lysates, cells were maintained with lysis buffer for 15 minutes on ice and centrifuged at 12,000 × g for 10 minutes. Samples containing total protein were separated by SDS-PAGE and transferred to nitrocellulose membranes. Membranes were blocked for one hour at room temperature (RT) with 5% non-fat powdered milk dissolved in TBS-Tween-20 (TBS-T) (50 mM Tris-Cl, pH 7.5; 150 mM NaCl; 0.1% Tween-20), incubated overnight (4°C) with primary antibodies and with secondary antibodies against mouse or rabbit IgG conjugated with peroxidase (Amersham) for one hour at RT. The membranes were washed three times with TBS-T, and incubated with the SignalFire ECL Reagent (Cell Signaling Technology) for protein bands visualization. The band's densitometry was performed using ImageJ software v1.53 (National Institutes of Health). The following antibodies were used: anti-PCNA (#2586); anti-γH2AX (#9718); anti-β-actin (#4967) (Cell Signaling), anti-α-tubulin (CP06) (Calbiochem), anti-N (MA5-35943) (Invitrogen), anti-laminA/C (#A303-430A) (Bethyl) and anti-FLAG (#A2220) (Sigma).

Immunohistochemistry

Lung tissue sections, obtained *via* Minimally Invasive Autopsies, (COVID-19 case and a control lung tissue of a non-smoker subject) were stained in silanized slides (Sigma Chemical Co. St. Louis, Missouri, EUA). Briefly, the histological sections were deparaffinized in xylene, rehydrated through a graded series of ethanol, and kept in a tri-phosphate buffer (TBS) pH 7.4. After deparaffinization, slides were hydrated for five minutes in graded alcohol series (100%, 95%, 70%, and H_2O) and incubated in Tris-EDTA for 50 minutes at 95°C pH 9.0. The blockage of the endogenous peroxidases was done by hydrogen peroxide 10v (3%).

The slides were then incubated with Ab mix (TBS (1%), BSA (4%), and Tween20 (0.02%)) for 20 minutes at RT followed by treatment overnight at 4°C with anti- γ-H2AX (Cell Signaling #9718S) diluted 1:500 in Ab mix or anti-PCNA diluted 1:1000 (DAKO #M0879). The slides were then washed twice in TBS (1%) and finally incubated for one hour at RT with 1:500 goat anti-rabbit/mouse HRP polymer detection kit – ImmunoHistoprobe Plus (ADVANCED-BIOSYSTEMS) for 30 minutes at 37°C). The diaminobenzidine (DAB) was used as a chromogen (Sigma-Aldrich Chemie, Steinheim, Germany). Finally, the counterstaining was done with Harris Hematoxylin (Merck,

Darmstadt, Germany), and the slides were mounted with a coverslip in Permount (Fischer #SP15-500). The use of this material for research purposes has been previously approved by the Institutional Ethical Board CAAE #30364720.0.0000.0068).

Anti-Viral *In Vitro* Efficacy Assay

Lung tissue sections A plaque assay was performed as described in Kashyap et al. (2021). Briefly, after seeding, Vero E6 (8×10^5 cells per well, 6-well plates) were incubated overnight and infected with 200 PFU per well. PCNA-I1 (Cayman #20454) or Verdinexor (Cayman #26171) were added at final concentrations of 0.5 μM or 0.1 μM and 0.1 μM or 1 μM, (Lu and Dong, 2019) in overlays composed of DMEM supplemented with 10% FBS plus carboxymethylcellulose sodium salt (Sigma-Aldrich #C5678) 2%, immediately post-viral adsorption. A MTT cell proliferation assay (Roche #11465007001) was done to verify the toxicity of the drugs (**Supplementary Figure S5**). After four days, cells were fixed with formaldehyde and stained with crystal violet to count plaques.

Statistical Analysis

Data are presented as mean ± Standard Deviation (SD). Statistical analysis of the data was performed by Student's t-test or ANOVA. P-values of ≤0.05 were considered statistically significant. All experiments were performed in biological duplicates. The odds ratio was calculated to verify if the translocation of the PCNA to the cytoplasm was dependent on the M transfection. A total of 147 cells were analyzed. A value of odds ratio greater than one indicates that the event observed is dependent on the object analyzed.

RESULTS

SARS-CoV-2 Structural Proteins Interact With PCNA in HEK293T Cells

In the study by Gordon et al. (2020), the interactome of the structural and non-structural proteins of SARS-CoV-2 was performed in HEK293T cells (Gordon et al., 2020). The analysis of affinity-purification–mass spectrometry (AP-MS)-based proteomics showed that PCNA interacts with E and M SARS-CoV-2 proteins. In our study, we validated this interaction through an anti-FLAG immunoprecipitation assay (**Figure 1A**). FLAG-tagged GFP, E, M, and N proteins were expressed in HEK293T cells and immunoprecipitated with anti-FLAG antibodies. As a result, we identified that PCNA co-immunoprecipitated with the E and M SARS-CoV-2

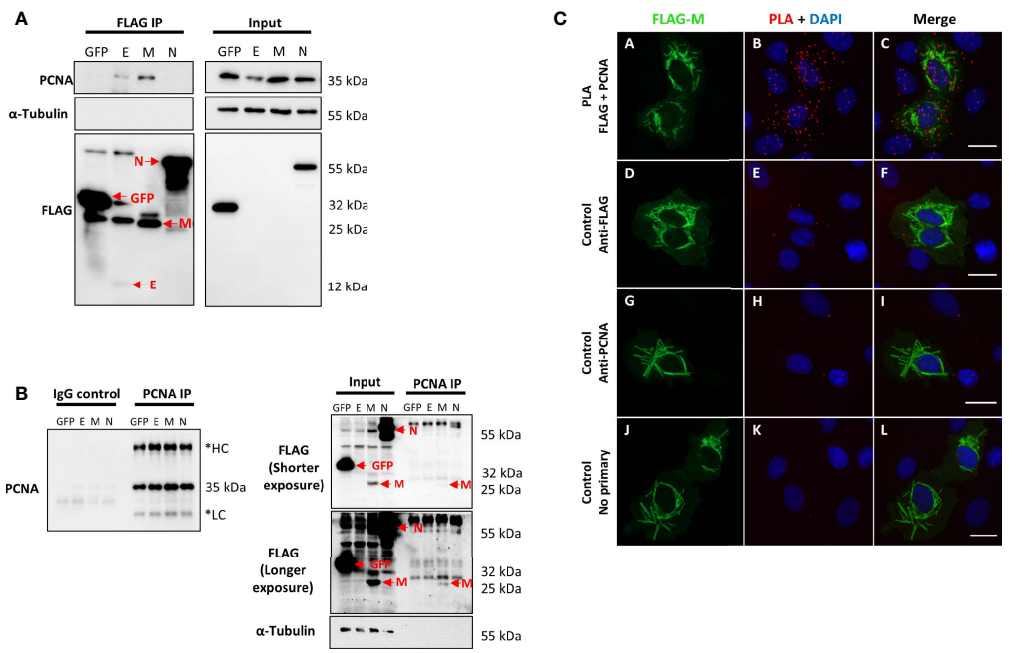

FIGURE 1 | SARS-CoV-2 structural proteins interact with PCNA in HEK293T and Vero E6 cells. FLAG-tagged GFP, E, M, and N proteins (indicated at the top of the panel) were expressed by transfection in HEK293T cells. Immunoprecipitation with anti-FLAG **(A)** or anti-PCNA antibodies **(B)** was performed (indicated on the panel's top). Blots were done with the primary antibodies indicated on the panel's left, and molecular weight markers sizes are indicated on the right. **(A)** PCNA was identified as an interactor of SARS-CoV-2 E and M proteins. **(B)** Immunoprecipitation of endogenous PCNA confirmed that protein M co-immunoprecipitated with PCNA. These data were obtained in one biological replicate. *HC, Heavy Chain; LC, Light chain. Red arrows indicate specific bands. **(C)** Vero E6 cells were transfected with pFLAG-M and submitted to ice-cold methanol fixation after 24h, followed by incubation with the primary antibodies, as indicated on the left, and PLA staining protocol. Panels **(A–C)** show positive PLA dots for FLAG and PCNA staining in transfected cells. Little to no signal is detected in the respective controls omitting one or both primary antibodies [panels **(D–L)**]. Images are representative of two independent experiments. Nuclei were stained with DAPI. All images were taken at 63× magnification with a ZEISS Axio Vert.A1 microscope.

proteinsbut not with the N protein, which is expected since PCNA was not identified as an interactor of N protein (Gordon et al., 2020). Anti-FLAG immunoprecipitation confirmed the interaction between M and PCNA in two independent experiments (**Supplementary Figure S1**). We also confirmed that PCNA and M interact, through a reverse immunoprecipitation assay (**Figure 1B**), in HEK293T cells previously transfected with FLAG-tagged GFP, E, M, and N. We identified that only FLAG-tagged M co-immunoprecipitated with PCNA, revealing a more specific interaction between these proteins. Furthermore, we explored the interaction between FLAG-M and PCNA by proximity ligation assay (PLA). Vero E6 cells expressing FLAG-M were fixed 24 h.p.t. (hours post-transfection) and labeled with primary antibodies against FLAG (rabbit) and PCNA (mouse), followed by PLA probes conjugated to anti-rabbit or anti-mouse. PLA signal is emitted when probes attached to primary antibodies are closer than 40 nm, indicating protein interaction. As negative controls, transfected cells were labeled with only one of the primary antibodies or omitting both. **Figure 1C** (panels A-C and **Supplementary Figure S2**) shows positive PLA dots in transfected cells, while minimal or no signal is seen in the respective controls (**Figure 1C** – panels D-L). Confocal microscopy analysis of the PLA assay also showed that the M-PCNA interaction occurs in the cytoplasm, indicating a possible translocation of the PCNA to the cytoplasm, induced by the M protein (**Supplementary Figure S3**).

SARS-CoV-2 M Expression in Vero E6 Cells Induces PCNA Translocation to the Cytoplasm

To better understand how the interaction of M-PCNA could be acting on the cells, we conducted immunofluorescence (IF) assays in Vero E6 cells expressing FLAG-M. 24 hours after transfection, cells were stained and analyzed by widefield microscopy (**Figure 2A**). Although PCNA did not entirely co-localize to the structures where M is present, we observed that in transfected cells, PCNA presented a more cytosolic pattern when compared to the non-transfected ones, as indicated by plot profile analysis (**Figure 2A** – Arrows 1 and 2). To further investigate this phenomenon, we quantified the fluorescence intensities of nuclear and cytoplasmic PCNA in cells expressing FLAG-M and non-transfected cells. **Figure 2B** shows that in non-transfected cells, PCNA has a propensity to be nuclear, but under FLAG-M expression, the PCNA is translocated to the cytoplasm. We also evaluated the translocation of PCNA to the cytoplasm by odds ratio. The odds ratio for cytoplasmic PCNA with FLAG-M expression was 6.34 (Confidence Interval 95% =2.83-13.3) compared to non-transfected cells, indicating the correlation of M protein with the translocation of the PCNA to the cytoplasm. In addition, the subcellular fractionation of Vero E6 cells transfected with FLAG-M or FLAG-GFP was carried out (**Figure 2C**). In agreement with IF data, FLAG-M transfected cells showed an evident reduction of PCNA in the nuclear fraction, while it remained nuclear in cells expressing FLAG-GFP (**Figure 2C**).

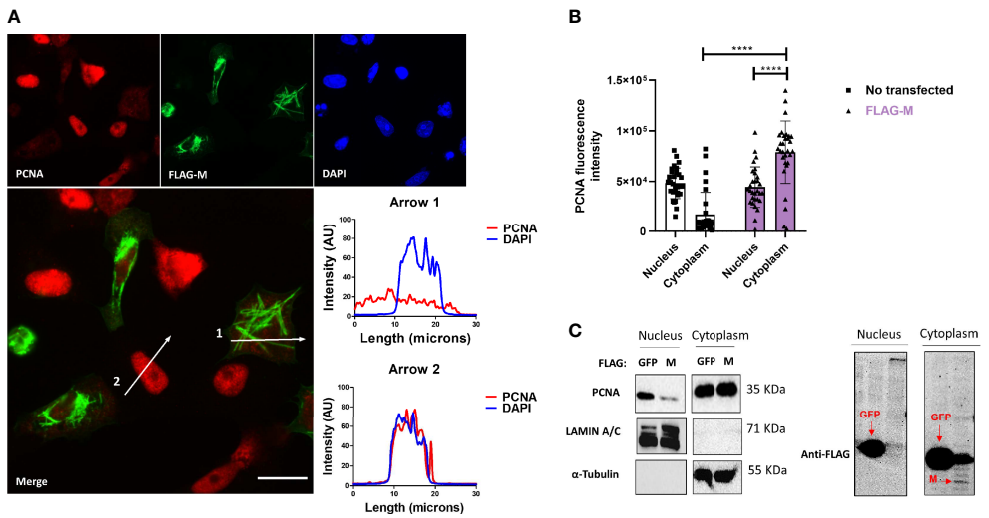

FIGURE 2 | FLAG-M expression promotes PCNA translocation to cytoplasm. **(A)** Vero E6 cells expressing FLAG-M protein, 24h after transfection, were fixed and stained for FLAG-M (green), PCNA (red), and DAPI. Graphs show plot profile intensities for PCNA and DAPI channels in the cross-sections indicated by arrows 1 and 2. Images are representative of two independent experiments. Scale bar 20 μm. **(B)** PCNA localization was analyzed through fluorescence intensity in non-transfected and FLAG-M transfected cells. Briefly, the nuclei area stained with DAPI was selected manually and the ROI (region of interest) obtained was used to measure PCNA intensities on nucleus and cytoplasm. Fluorescence intensity was quantified in grayscale on ImageJ. This data is representative of two independent experiments. The data represent mean ± SD (n=30). For statistical analysis, Two-way ANOVA and multiple comparison Bonferroni's tests were used. ****$p < 0.0001$ were considered statistically significant. **(C)** Vero E6 cells were transfected with vectors to express FLAG-tagged M or GFP proteins, and after 48 hours cellular fractionation followed by Western blotting was performed. LAMIN A/C and α-Tubulin proteins were used as controls for nuclear and cytosolic fractions, respectively. The expression of the transfected proteins is shown in the right panel. Western blot images are representative of one independent experiment.

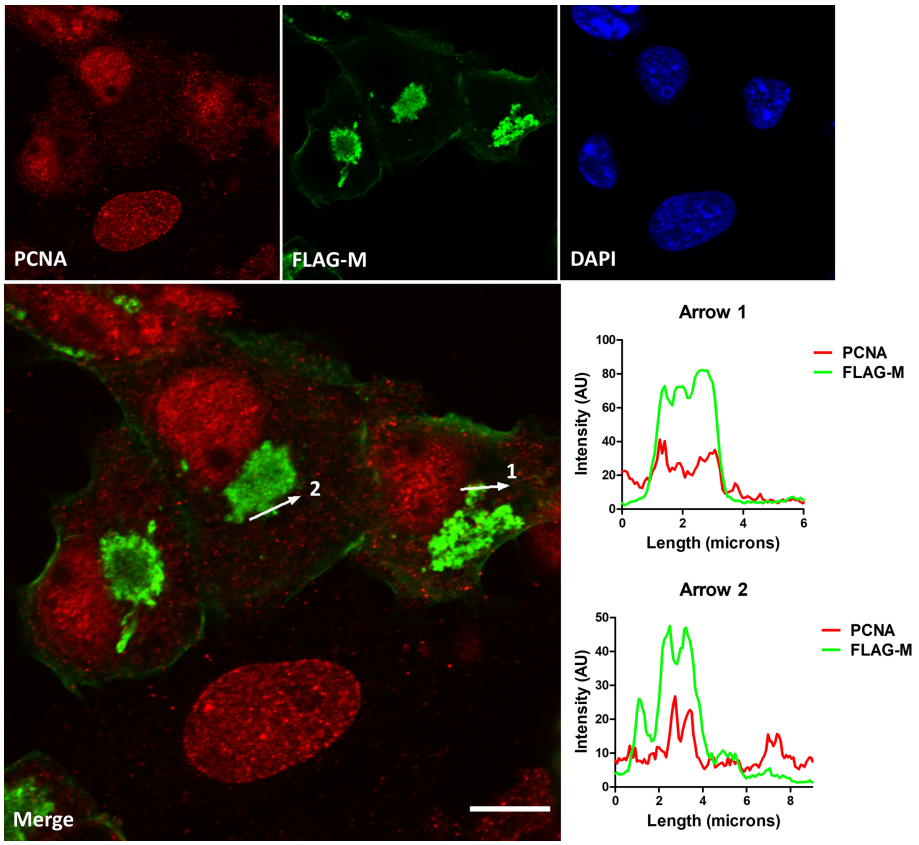

FIGURE 3 | Co-localization of FLAG-M and PCNA by confocal immunofluorescence. Vero E6 cells expressing FLAG-M and stained for PCNA (red) and FLAG-M (green) were analyzed by confocal microscopy. The plot profile of two arrowed areas (arrows 1 and 2) indicates an overlap in signals of both proteins, as shown in the graphs on the right. Images were taken at 100× magnification with a Zeiss LSM-780-NLO microscope. Scale bar 10 μm.

These results indicate that M protein acts on PCNA translocation from the nucleus to the cytoplasm.

SARS-CoV-2 M Protein Interacts With PCNA in the Cytoplasm of Vero E6 Cells

To confirm the interaction between M and PCNA, we performed confocal immunofluorescence of FLAG-M transfected cells. Plot profile analysis shows an overlap between FLAG-M and PCNA signals, indicating the proximity of the proteins (**Figure 3**). Moreover, as mentioned before, the interaction between FLAG-M and PCNA was detected by PLA (**Figure 1C**), and the co-localization of PLA puncta with FLAG-M was shown by confocal microscopy (**Supplementary Figure S3**). Taken together, these results indicate the ability of M protein in inducing PCNA translocation from the nucleus, and to interact with it in the cytoplasm.

FLAG-M Expression Increases DNA Damage Marker Levels in HEK293T and Vero E6 Cells

PCNA is one of the essential proteins for DNA replication and DNA repair, and it is also known as a DNA damage marker. To address whether M expression could be related to the induction of DNA damage. We transfected HEK293T and Vero E6 cellswith FLAG-M and looked at γH2AX and PCNA expression levels since both proteins elevated expression is associated with DNA damage. In HEK293T transfected cells, we could observe a slight increase in the levels of PCNA and γH2AX (**Figure 4A**), but no significant difference was observed in the Vero E6 cell line (**Figure 4B**). Because transfection efficiency could be a limiting factor for detecting inconspicuous events like DNA damage, we also explored γH2AX levels in transfected Vero E6 cells by immunofluorescence (**Figure 4C**). Comparing the γH2AX fluorescence intensity in FLAG-M transfected cells with non-transfected cells, we found a significant increase in the phosphorylation level of H2AX, suggesting that M involvement with PCNA may promote DNA damage (**Figure 4D**).

SARS-CoV-2 Infection Induces PCNA Translocation to the Cytoplasm and Promotes DNA Damage

To verify if our findings concerning M protein and the DNA damage markers PCNA and γH2AX were also reproducible during infection, we evaluated the effect of SARS-CoV-2 infection in Vero E6 cells. Immunofluorescence analysis

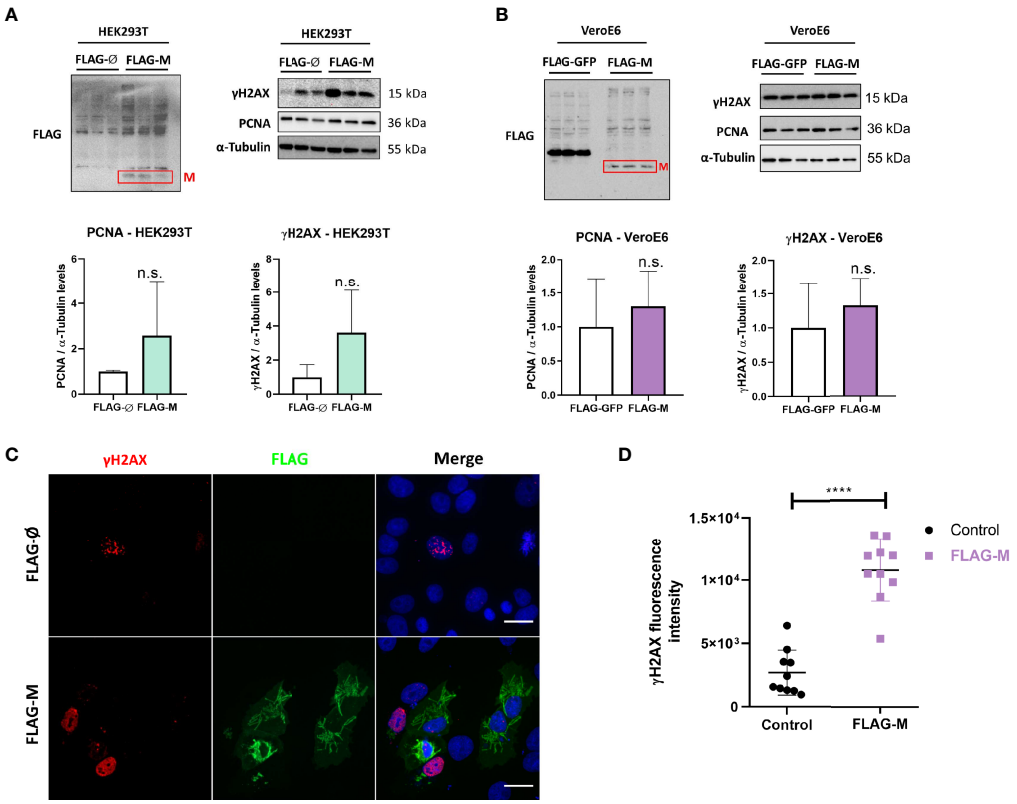

FIGURE 4 | PCNA and γH2AX levels in transfected cell lines. **(A)** Detection of PCNA and γH2AX levels in HEK293T cells transfected with pFLAG-M compared to pFLAG (empty vector). **(B)** Detection of PCNA and γH2AX levels in Vero E6 cells transfected with pFLAG-M compared to pFLAG-GFP. Graphs show a slight increase in normalized protein levels; however, the statistical test does not show significance. Western blotting data in **(A, B)** are representative of one independent experiment. **(C)** Immunofluorescent staining of FLAG-M (green) and γH2AX (red) in Vero E6 cells 24 hours post-transfection. Images are representative of two independent experiments. Scale bar 20 μm. **(D)** Fluorescence intensity quantification of γH2AX levels in FLAG-M transfected versus non-transfected cells. Fluorescence intensities in the nucleus were measured as described in **Figure 2B**. Data represent mean ± SD in samples from 2 independent experiments (n = 10). For statistical analysis, a two-tailed unpaired T-test was conducted. n.s, non-significant, ****$p < 0.0001$ was considered statistically significant.

showed PCNA staining in the cytoplasm of infected cells, with PCNA presenting mainly a nuclear pattern on mock control (**Figure 5A**). The results (**Figures 5B, C**) show a higher intensity of PCNA in the cytoplasm of infected cells with a concomitant reduction in its nuclear signal compared to mock-infected cells. In addition, a higher γH2AX fluorescence intensity was observed in infected cells compared to non-infected cells, which confirms that the infection promotes DNA damage (**Figures 5D, E**). We also evaluated PCNA and γH2AX levels by western blotting in HEK293T and Vero E6 infected cells (**Figure 5F**). The effect observed during infection is a higher expression of PCNA and phosphorylation of histone H2AX in both cell lines (**Figures 5G, H**).

We then compared PCNA (top panels) and γH2AX (bottom panels) expression levels in lung sections obtained from control and COVID-19 patients through immunohistochemistry assay (**Supplementary Figure S4**). Our results indicate high expression of both markers in COVID-19 patient (right panels), suggesting the involvement of both PCNA and γH2AX in SARS-CoV-2 infection *in vivo*.

Stabilization of PCNA Trimer by PCNA-I1 or Blockage of CRM-1 Transporter by Verdinexor Inhibits SARS-CoV-2 Replication

Our data indicate that PCNA translocates to the cytoplasm after M protein expression or SARS-CoV2 infection. To analyze if this phenomenon plays a role in the replicative cycle of the virus, two inhibitors of this transport were used to prevent the PCNA migration to the cytoplasm and test their possible anti-viral activity. The inhibitor of PCNA (PCNA I1) prevents the transportation of the PCNA to the cytoplasm by stabilizing its trimer form in the nucleus. Verdinexor is a selective inhibitor of nuclear export protein exportin-1 (XPO1), also called Chromosome Region Maintenance 1(CRM1), and was already described as essential in the PCNA translocation (Bouayad et al., 2012; Perwitasari et al., 2016). Vero E6 cells were tested for PCNAi and Verdinexor toxicity, showing that 10 to 0.1 μM are safe concentrations for both drugs, since they did not reduce cells viability (**Figure S5**). Vero E6 cells were then infected and submitted to a dose-dependent anti-viral *in vitro* efficacy assay.

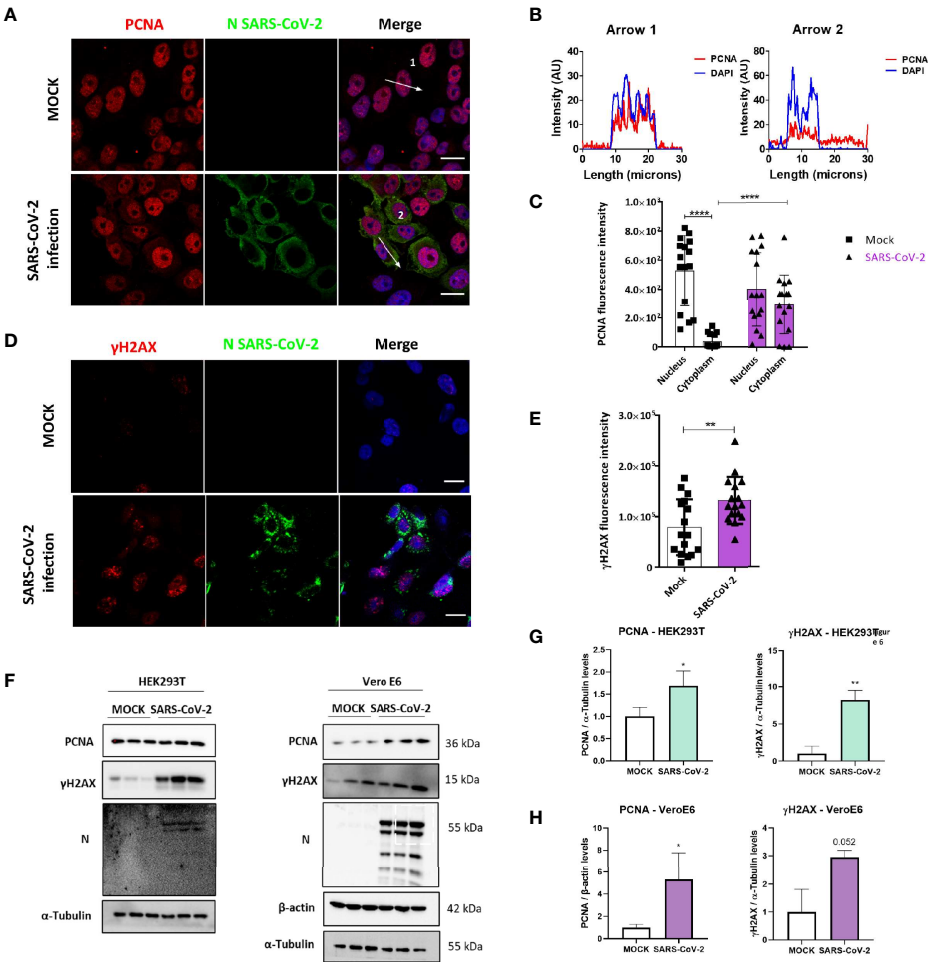

FIGURE 5 | SARS-CoV-2 infection promotes PCNA translocation to the cytoplasm and enhances PCNA and γH2AX expression. **(A)** Vero E6 cells were infected with SARS-CoV2 (MOI 0.3), and 24 hours post-infection immunofluorescence was performed for N (green) and PCNA (red). Scale bars 20 μm. **(B)** Plot profile intensities for PCNA and DAPI channels in the cross-sections, indicated by arrows 1 and 2. Images are representative of two independent experiments. Scale bar 20 μm. **(C)** PCNA localization was analyzed through fluorescence intensity mock versus infected cells, as described in **Figure 2B**. White bars = mock, purple bars = SARS-CoV-2 infection. **(D)** Vero E6 cells were infected with SARS-CoV2 (MOI 0.3), and 24 hours post-infection immunofluorescence was performed for N (green) and γH2AX (red). Scale bars 20 μm. **(E)** Fluorescence intensity of γH2AX in the nucleus was analyzed in mock and infected cells, as described in **Figure 2B**. White bars = mock, purple bars = SARS-CoV-2 infection. **(F)** Western blotting analysis of PCNA and γH2AX levels in HEK293T and Vero E6 cells infected with SARS-CoV-2 compared to mock. Statistical analysis for normalized expression levels of PCNA and γH2AX are shown for HEK293T **(G)** and Vero E6 cells **(H)**. Data represent means ± SD from 1 independent experiment. For fluorescence intensity (n = 20), data were analyzed by Two-way ANOVA and multiple comparisons Bonferroni's test. *p < 0.05 and ****p < 0.0001 were considered statistically significant **p < 0.01.

The results (**Figure 6**) indicate that PCNAi 0.5 μM and Verdinexor 0.1 μM have the best effects against SARS-CoV-2, reducing the viral replication roughly by 20% and 15%, respectively, compared to the DMSO.

DISCUSSION

After nearly two years since the start of the COVID-19 pandemic, understanding the underlying mechanisms of SARS-CoV-2 infection and the search for treatment are still in high demand. Large-scale analysis of SARS-CoV-2 human infection interactome indicated several protein-protein interactions that require further validation (Bouhaddou et al., 2020; Gordon et al., 2020; Li et al., 2021; Stukalov et al., 2021). In this work, we aimed to characterize the interactions of viral proteins and PCNA. According to Gordon et al. (2020), the score of SAINT probability of PCNA for E protein was zero (a low score of interaction probability), and for M was 1.0 (a high score of interaction probability), while PCNA did not appear as an interactor for N protein. Through immunoprecipitation and PLA assays (**Figure 1**), we validated the M-PCNA interaction. The E-PCNA interaction was not detected in the reverse immunoprecipitation (PCNA pull down, **Figure 1B**), and we focused on the M-PCNA interaction.

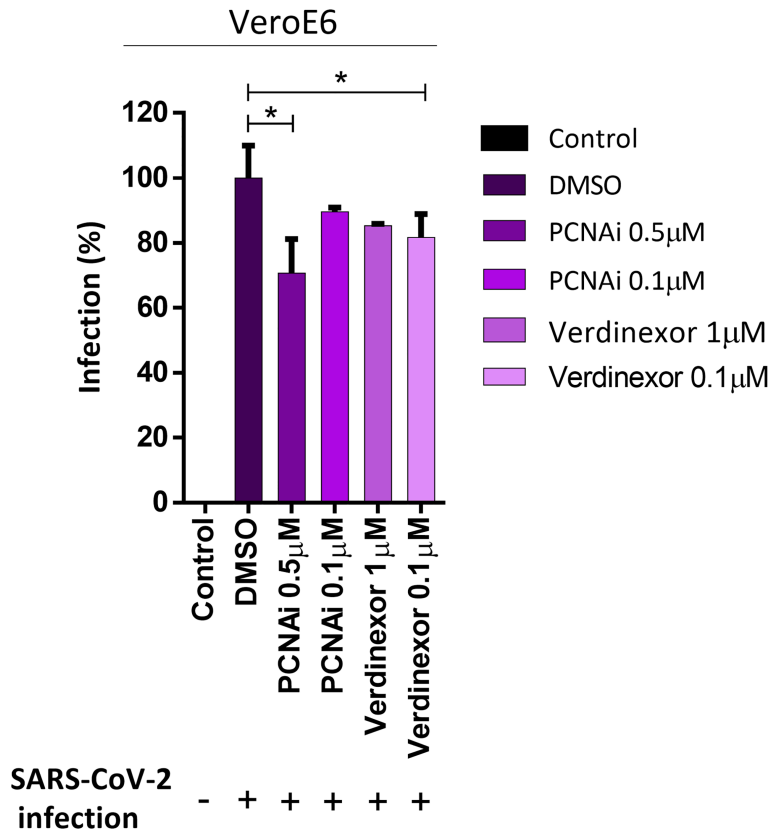

FIGURE 6 | PCNA I1 and Verdinexor inhibit SARS-CoV-2 viral replication *in vitro*. Vero E6 cells were infected with SARS-CoV-2 as described in the anti-viral *in vitro* efficacy assay (see Methods), for one hour, then DMSO, PCNA I1 0.5 and 0.1 μM or Verdinexor 1 and 0.1 μM were added to overlay media one hour after virus adsorption. The viral load was assessed by plaque assay after four days of incubation. This data is representative of two independent experiments. T-test was used for independent comparisons between DMSO versus PCNA I1, and DMSO versus Verdinexor. *$p < 0.05$ were considered statistically significant.

PLA assay indicates that M-PCNA interaction occurs in the cytoplasm (**Figure 1C**), and to better characterize it, we performed a co-localization assay by immunofluorescence and subcellular fractioning. Our data indicate that in M expression (**Figure 2**) or upon SARS-CoV-2 infection (**Figures 5A-C**), PCNA translocates from nucleus to cytoplasm. In agreement with PLA data, upon M expression there is also a partial co-localization among M and PCNA in the cytoplasm documented by confocal microscopy (**Figure 3** and **Supplementary Figure S3**). This can be hypothesized as a need for the virus to have PCNA partially translocated from the nucleus to the cytoplasm, and that M is responsible, at least in part, for this translocation in the context of the viral infection.

PCNA acts as a co-factor for DNA polymerases in normal conditions, being essential for DNA replication (O'Donnell et al., 2013; Siddiqui et al., 2013). PCNA also participates in DNA repair, on the metabolism of DNA, and chromatin by recruiting various enzymes, and not only by acting as a scaffold and localizing these factors, but also activating their enzymatic activities (Choe and Moldovan, 2017). Aside from this, post-translational modifications in PCNA alter its function in different ways (Hoege et al., 2002; Moldovan et al., 2007; Choe and Moldovan, 2017). The interactome described by Stukalov et al. (2021) demonstrated that higher ubiquitination occurs in specific regions of PCNA in SARS-CoV-2 infection, indicating a regulatory mechanism of PCNA by the virus infection (Stukalov et al., 2021).

In cells transfected with FLAG-M (**Figure 4**) or infected with SARS-CoV-2, we observed an increase of PCNA and γH2AX (**Figures 5D–H**), and both proteins are associated with DNA repair. We also found a high expression of PCNA and γH2AX in a COVID-19 patient (**Figure S4**). Li et al. (2021) already reported a high PCNA expression in moderate COVID-19 patients compared to the control group by proteomics analysis (Li et al., 2021). It has been reported that virus infection in human cells can cause DNA damage, inhibiting the association of the DNA polymerase to the DNA stalling and collapsing the replication forks, which results in DNA double-strand breaks (DSB) (Kannouche et al., 2004; Luftig, 2014). This damage activates a stress response, mediated by checkpoint kinases, which help stabilize and restart the replication forks, thus preventing the generation of DNA damage and genomic instability (Zeman and Cimprich, 2014). In this case, one of the strategies of the cells is to trigger the PCNA ubiquitination.

When PCNA is polyubiquitinated, it searches for damaged DNA to assemble the replication complex, with a less specific DNA polymerase (Boehm et al., 2016). This mechanism is known as translesion synthesis (TLS) and is activated to bypass damaged DNA (Kannouche et al., 2004). Thus, the increase of PCNA could be a strategy for the viral infection to maintain cell viability. Also, after DNA damage, several proteins are activated to manage the DNA lesion. One of them is γH2AX, the phosphorylated form of H2AX, a specific marker of DNA damage that is responsible for recruiting repair proteins to deal with stalled forks (Dickey et al., 2009; Choe et al., 2016), and also increases the expression of p53 and phosphorylation of p53, leading to cell growth inhibition (Dillehay et al., 2014; Dillehay et al., 2015).

PCNA is also found in the cytoplasm of cancer cells. The accumulation of PCNA in the cytoplasm of cancer cells evidenced interactions between PCNA and the proteins in the cytoplasm (Byung and Lee, 2006). PCNA can bind to enzymes of the glycolysis pathway and regulate energy production in the mitochondria; maintain cytoskeleton integrity; and participate in other signaling pathways (Neuman et al., 2011; Bouhaddou et al., 2020). Li et al. (2021) described that SARS-CoV-2 M protein has its activity connected to ATP biosynthesis and metabolic processes (Li et al., 2021). Considering these data, the PCNA translocation from the nucleus to cytoplasm reported here may also be associated with the regulation of metabolism in infected cells to maintain SARS-CoV-2 replication.

Another hypothesis is that cytosolic PCNA, in association with the M protein, could bind to proteins that inhibit the immune response. Several studies pointed out that cytoplasmic PCNA is found in mature neutrophils associated with procaspases, thus preventing neutrophils from apoptosis (Witko-Sarsat et al., 2010). The accumulation of PCNA in the cytoplasm of mature neutrophils is due to the activity of the chromosome region maintenance 1 (CRM1)-dependent nuclear-to-cytoplasmic relocalization during granulocytic (Bouayad et al., 2012). Cytoplasmic PCNA is also associated with Caspase-9 in the SH-SY5Y neuroblastoma cell line, and S-nitrosylation of PCNA at the residues C81 and C162 decreases this interaction, leading to caspase-9 activation (Yin et al., 2015).

Verdinexor is a selective inhibitor of nuclear export (SINE), a molecular drug that binds to CRM-1 and blocks the transport of proteins from the nucleus to the cytoplasm, including PCNA (Bouayad et al., 2012; Widman et al., 2018). The CRM-1 inhibitors have demonstrated activity against over 20 different DNA and RNA viruses, including influenza and respiratory syncytial virus (Perwitasari et al., 2014; Widman et al., 2018; Jorquera et al., 2019). In addition, Selinexor, another SINE, reduced SARS-CoV-2 infection *in vitro* and protected the respiratory system in an *in vivo* model (Kashyap et al., 2021). We found that Verdinexor 0.1 μM was a safe dose and enough to reduced viral replication by 15% (**Figure 6**), corroborating the previous SINE study. Nonetheless, SINEs are drugs that could act in the translocation of different proteins, not only in PCNA. We also treated cells with different doses of PCNA inhibitor (PCANI1). This inhibitor stabilizes the PCNA trimer and prevents the PCNA translocation from the nucleus to the cytoplasm and reallocation inside the nucleus (Lu and Dong, 2019). This inhibits the PCNA action on the replication forks and indirectly leads tumor cells to a higher sensitivity to anticancer DNA damaging drugs (Klein et al., 2020; Wyler et al., 2020). Our results show that PCNA I1 0.5 μM reduced viral replication by 20% (**Figure 6**), no difference was seen when the cells were treated with PCNA I1 0.1 μM. Our results indicate a potential use of PCNA and nuclear translocation inhibitors as treatments for COVID-19.

CONCLUSIONS

The SARS-CoV-2 virus can manipulate many pathways to replicate in the host cell. In this study, we validated the PCNA-M interaction and underlined some of the potential mechanisms regarding this interaction. The increase of the PCNA and γH2AX levels in the nucleus may prolong cell viability to favor virus replication. On the other hand, the translocation of PCNA and its association with M in the cytoplasm may manipulate the immune response and regulate cell metabolism to favor virus replication. Finally, inhibition of PCNA translocation from the nucleus to cytoplasm reduced the formation of plaques in an *in vitro* assay, indicating a potential therapeutic target. The original data reported here may help to better understand the SARS-CoV-2 replication mechanisms, thus impacting therapeutic strategies for COVID-19 resolution.

DATA AVAILABILITY STATEMENT

The datasets presented in this study can be found in online repositories. The names of the repository/repositories and accession number(s) can be found in the article/**Supplementary Material**.

ETHICS STATEMENT

The studies involving human participants were reviewed and approved by Institutional Ethical Board CAAE #30364720.0.0000.0068. The patients/participants provided their written informed consent to participate in this study.

AUTHOR CONTRIBUTIONS

Conceptualization, FS and AV; methodology, ÉZ, IP, MM, AM, MS, OS, MG, KS, and MA; software, MS; validation, ÉZ, IP, MM, AM, MS, OS, and MG; formal analysis, ÉZ, FS, HM-S and AV; investigation, ÉZ and FS; resources, FS, JP-M, HM-S, TM, MD, PS, and AV; data curation, ÉZ, MM, MS, FS, HM-S, and AV; writing original draft preparation, ÉZ; writing—review and editing, ÉZ, FS, JP-M, and AV; visualization, ÉZ, IP, MM, AM, MS, OS, MG, KS, MA, DT-T, and PP; supervision, FS, JP-M, HM-S, and AV; project administration, FS and JP-M; funding

acquisition, FS and JP-M. All authors have read and agreed to the published version of the manuscript.

FUNDING

This work was supported by grants from FAEPEX-UNICAMP (2005/20; 2319/20; 2432/20; 2274/20; 2266/20), Fundação de Amparo à Pesquisa do Estado de São Paulo (FAPESP), grant numbers 2020/05346-6, 2018/14818-9, 2020/04558-0 and 2016/00194-8. JP-M is supported by Conselho Nacional de Desenvolvimento Científico e Tecnológico (CNPq) grant no number 305628/2020-8.

ACKNOWLEDGMENTS

We acknowledge the students that helped ÉZ during the cell lines infection in the Biosafety Level 3 Laboratory (NB3) and all others that were our backup outside of the lab. We thank the UNICAMP-Task-Force against COVID-19 that facilitated this study.

SUPPLEMENTARY MATERIAL

The Supplementary Material for this article can be found online at: https://www.frontiersin.org/articles/10.3389/fcimb.2022.849017/full#supplementary-material

REFERENCES

Alharbi, S. N., and Alrefaei, A. F. (2021). Comparison of the SARS-CoV-2 (2019-Ncov) M Protein With its Counterparts of SARS-CoV and MERS-CoV Species. *J. King Saud. Univ. - Sci.* 33, 101335–101344. doi: 10.1016/j.jksus.2020.101335

Amaral, C. L., Freitas, L. B., Tamura, R. E., Tavares, M. R., Pavan, I. C. B., Bajgelman, M. C., et al. (2016). S6Ks Isoforms Contribute to Viability, Migration, Docetaxel Resistance and Tumor Formation of Prostate Cancer Cells. *BMC Cancer* 16, 602. doi: 10.1186/s12885-016-2629-y

Baldwin, (1996). Nuclear & Cytoplasmic Extract Protocol. *Ann. Rev. Immunol.* 14, 649–681. doi: 10.1146/annurev.immunol.14.1.649

Boehm, E. M., Gildenberg, M. S., and Washington, M. T. (2016). The Many Roles of PCNA in Eukaryotic Dna Replication. *EnzymesI* 39, 231–254. doi: 10.1016/bs.enz.2016.03.003

Bojkova, D., Klann, K., Koch, B., Widera, M., Krause, D., Ciesek, S., et al. (2020). Proteomics of SARS-CoV-2-infected Host Cells Reveals Therapy Targets. *Nature* 583, 469–472. doi: 10.1038/s41586-020-2332-7

Bouayad, D., Pederzoli-Ribeil, M., Mocek, J., Candalh, C., Arlet, J. B., Hermine, O., et al. (2012). Nuclear-to-Cytoplasmic Relocalization of the Proliferating Cell Nuclear Antigen (PCNA) During Differentiation Involves a Chromosome Region Maintenance 1 (CRM1)-Dependent Export and is a Prerequisite for PCNA Antiapoptotic Activity in Mature Neutrophils. *J. Biol. Chem.* 287, 33812–33825. doi: 10.1074/jbc.M112.367839

Bouhaddou, M., Memon, D., Meyer, B., White, K. M., Rezelj, V. V., Correa Marrero, M., et al. (2020). The Global Phosphorylation Landscape of SARS-CoV-2 Infection. *Cell* 182. doi: 10.1016/j.cell.2020.06.034

Byung, J. K., and Lee, H. (2006). Importin-β Mediates Cdc7 Nuclear Import by Binding to the Kinase Insert II Domain, Which can be Antagonized by Importin-α. *J. Biol. Chem.* 281, 12041-12049. doi: 10.1074/jbc.M512630200

Chen, N., Zhou, M., Dong, X., Qu, J., Gong, F., Han, Y., et al. (2020). Epidemiological and Clinical Characteristics of 99 Cases of 2019 Novel Coronavirus Pneumonia in Wuhan, China: A Descriptive Study. *Lancet* 395, 30211–30217. doi: 10.1016/S0140-6736(20)30211-7

Choe, K. N., and Moldovan, G. L. (2017). Forging Ahead Through Darkness: Pcna, Still the Principal Conductor at the Replication Fork. *Mol. Cell* 65, 380–392. doi: 10.1016/j.molcel.2016.12.020

Choe, K. N., Nicolae, C. M., Constantin, D., Imamura Kawasawa, Y., Delgado-Diaz, M. R., De, S., et al. (2016). HUWE 1 Interacts With PCNA to Alleviate Replication Stress. *EMBO Rep.* 17, 874-886. doi: 10.15252/embr.201541685

Dickey, J. S., Redon, C. E., Nakamura, A. J., Baird, B. J., Sedelnikova, O. A., and Bonner, W. M. (2009). H2ax: Functional Roles and Potential Applications. *Chromosoma* 118, 683–692. doi: 10.1007/s00412-009-0234-4

Dillehay, K. L., Lu, S., and Dong, Z. (2014). Antitumor Effects of a Novel Small Molecule Targeting PCNA Chromatin Association in Prostate Cancer. *Mol. Cancer Ther.* 13, 2817–2826. doi: 10.1158/1535-7163.MCT-14-0522

Dillehay, K. L., Seibel, W. L., Zhao, D., Lu, S., and Dong, Z. (2015). Target Validation and Structure-Activity Analysis of a Series of Novel PCNA Inhibitors. *Pharmacol. Res. Perspect.* 3, 2817–2826. doi: 10.1002/prp2.115

Fu, Y. Z., Wang, S. Y., Zheng, Z. Q., Huang, Y., Li, W. W., Xu, Z. S., et al. (2021). Sars-CoV-2 Membrane Glycoprotein M Antagonizes the MAVS-mediated Innate Antiviral Response. *Cell. Mol. Immunol.* 18, 613–620. doi: 10.1038/s41423-020-00571-x

Gordon, D. E., Jang, G. M., Bouhaddou, M., Xu, J., Obernier, K., White, K. M., et al. (2020). A SARS-CoV-2 Protein Interaction Map Reveals Targets for Drug Repurposing. *Nature* 583, 459–468. doi: 10.1038/s41586-020-2286-9

Hasan, S., and Hossain, M. M. (2020). Analysis of COVID-19 M Protein for Possible Clues Regarding Virion Stability, Longevity and Spreading. doi: 10.31219/osf.io/e7jkc

Hoege, C., Pfander, B., Moldovan, G. L., Pyrowolakis, G., and Jentsch, S. (2002). RAD6-Dependent DNA Repair Is Linked to Modification of PCNA by Ubiquitin and SUMO. *Nature* 419, 135–141. doi: 10.1038/nature00991

Hurst, K. R., Kuo, L., Koetzner, C. A., Ye, R., Hsue, B., and Masters, P. S. (2005). A Major Determinant for Membrane Protein Interaction Localizes to the Carboxy-Terminal Domain of the Mouse Coronavirus Nucleocapsid Protein. *J. Virol.* 79, 13285–13297. doi: 10.1128/jvi.79.21.13285-13297.2005

Jorquera, P. A., Mathew, C., Pickens, J., Williams, C., Luczo, J. M., Tamir, S., et al. (2019). Verdinexor (KPT-335), a Selective Inhibitor of Nuclear Export, Reduces Respiratory Syncytial Virus Replication *in Vitro*. *J. Virol.* 93, e01684–18. doi: 10.1128/jvi.01684-18

Kannouche, P. L., Wing, J., and Lehmann, A. R. (2004). Interaction of Human DNA Polymerase η With Monoubiquitinated PCNA: A Possible Mechanism for the Polymerase Switch in Response to DNA Damage. *Mol. Cell* 14, 491–500. doi: 10.1016/S1097-2765(04)00259-X

Kashyap, T., Murray, J., Walker, C. J., Chang, H., Tamir, S., Hou, B., et al. (2021). Selinexor, a Novel Selective Inhibitor of Nuclear Export, Reduces SARS-CoV-2 Infection and Protects the Respiratory System *In Vivo*. *Antiviral Res.* 192, 105115–105123. doi: 10.1016/j.antiviral.2021.105115

Klein, S., Cortese, M., Winter, S. L., Wachsmuth-Melm, M., Neufeldt, C. J., Cerikan, B., et al. (2020). Sars-CoV-2 Structure and Replication Characterized by *in Situ* Cryo-Electron Tomography. *Nat. Commun.* 11, 5885–5896. doi: 10.1038/s41467-020-19619-7

Kuo, L., Hurst-Hess, K. R., Koetzner, C. A., and Masters, P. S. (2016). Analyses of Coronavirus Assembly Interactions With Interspecies Membrane and Nucleocapsid Protein Chimeras. *J. Virol.* 90, 4357–4368. doi: 10.1128/jvi.03212-15

Lee, C.-C., Wang, J.-W., Leu, W.-M., Huang, Y.-T., Huang, Y.-W., Hsu, Y.-H., et al. (2019). Proliferating Cell Nuclear Antigen Suppresses RNA Replication of Bamboo Mosaic Virus Through an Interaction With the Viral Genome. *J. Virol.* 93, e00961–19. doi: 10.1128/jvi.00961-19

Li, J., Guo, M., Tian, X., Wang, X., Yang, X., Wu, P., et al. (2021). Virus-Host Interactome and Proteomic Survey Reveal Potential Virulence Factors Influencing Sars-CoV-2 Pathogenesis. *Med* 2, 99–112. doi: 10.1016/j.medj.2020.07.002

Li, C. K., Wu, H., Yan, H., Ma, S., Wang, L., Zhang, M., et al. (2008). T Cell Responses to Whole Sars Coronavirus in Humans. *J. Immunol.* 181, 5490–5500. doi: 10.4049/jimmunol.181.8.5490

Lu, S., and Dong, Z. (2019). Additive Effects of a Small Molecular PCNA Inhibitor PCNA-I1S and DNA Damaging Agents on Growth Inhibition and DNA Damage in Prostate and Lung Cancer Cells. *PloS One* 14, e0223894–0223904. doi: 10.1371/journal.pone.0223894

Luftig, M. A. (2014). Viruses and the DNA Damage Response: Activation and Antagonism. *Annu. Rev. Virol.* 1, 605–625. doi: 10.1146/annurev-virology-031413-085548

Lu, S., Ye, Q., Singh, D., Cao, Y., Diedrich, J. K., Yates, J. R., et al. (2021). The SARS-CoV-2 Nucleocapsid Phosphoprotein Forms Mutually Exclusive Condensates With RNA and the Membrane-Associated M Protein. *Nat. Commun.* 12, 502–514. doi: 10.1038/s41467-020-20768-y

Maga, G., and Hübscher, U. (2003). Proliferating Cell Nuclear Antigen (PCNA): A Dancer With Many Partners. *J. Cell Sci.* 116:3051–3060. doi: 10.1242/jcs.00653

Moldovan, G. L., Pfander, B., and Jentsch, S. (2006). Pcna Controls Establishment of Sister Chromatid Cohesion During S Phase. *Mol. Cell* 23, 723–732. doi: 10.1016/j.molcel.2006.07.007

Moldovan, G. L., Pfander, B., and Jentsch, S. (2007). PCNA, the Maestro of the Replication Fork. *Cell* 129, 665–679. doi: 10.1016/j.cell.2007.05.003

Naryzhny, S. N., and Lee, H. (2010). Proliferating Cell Nuclear Antigen in the Cytoplasm Interacts With Components of Glycolysis and Cancer. *FEBS Lett.* 584, 4292–4308. doi: 10.1016/j.febslet.2010.09.021

Naryzhny, S. N., Zhao, H., and Lee, H. (2005). Proliferating Cell Nuclear Antigen (PCNA) may Function as a Double Homotrimer Complex in the Mammalian Cell. *J. Biol. Chem.* 280, 13888–13894. doi: 10.1074/jbc.M500304200

Neuman, B. W., Kiss, G., Kunding, A. H., Bhella, D., Baksh, M. F., Connelly, S., et al. (2011). A Structural Analysis of M Protein in Coronavirus Assembly and Morphology. *J. Struct. Biol.* 174, 11–22. doi: 10.1016/j.jsb.2010.11.021

O'Donnell, M., Langston, L., and Stillman, B. (2013). Principles and Concepts of DNA Replication in Bacteria, Archaea, and Eukarya. *Cold Spring Harb. Perspect. Biol.* 5, a010108–010115. doi: 10.1101/cshperspect.a010108

Ohayon, D., De Chiara, A., Dang, P. M. C., Thieblemont, N., Chatfield, S., Marzaioli, V., et al. (2019). Cytosolic PCNA Interacts With p47phox and Controls NADPH Oxidase NOX2 Activation in Neutrophils. *J. Exp. Med.* 216 2669–2687. doi: 10.1084/jem.20180371

Olaisen, C., Müller, R., Nedal, A., and Otterlei, M. (2015). PCNA-Interacting Peptides Reduce Akt Phosphorylation and TLR-mediated Cytokine Secretion Suggesting a Role of PCNA in Cellular Signaling. *Cell. Signal.* 27, 1478–1487. doi: 10.1016/j.cellsig.2015.03.009

Oliveira, A. P., Simabuco, F. M., Tamura, R. E., Guerrero, M. C., Ribeiro, P. G. G., Libermann, T. A., et al. (2013). Human Respiratory Syncytial Virus N, P and M Protein Interactions in HEK-293T Cells. *Virus Res.* 177, 108–112. doi: 10.1016/j.virusres.2013.07.010

Opstelten, D. J. E., Raamsman, M. J. B., Wolfs, K., Horzinek, M. C., and Rottier, P. J. M. (1995). Envelope Glycoprotein Interactions in Coronavirus Assembly. *J.Cell Biol.* 131, 339–349. doi: 10.1083/jcb.131.2.339

Pang, H., Liu, Y., Han, X., Xu, Y., Jiang, F., Wu, D., et al. (2004). Protective Humoral Responses to Severe Acute Respiratory Syndrome-Associated Coronavirus: Implications for the Design of an Effective Protein-Based Vaccine. *J. Gen. Virol.* 85, 3109–3113. doi: 10.1099/vir.0.80111-0

Paunesku, T., Mittal, S., Protić, M., Oryhon, J., Korolev, S. V., Joachimiak, A., et al. (2001). Proliferating Cell Nuclear Antigen (PCNA): Ringmaster of the Genome. *Int. J. Radiat. Biol.* 77, 1007–1021. doi: 10.1080/09553000110069335

Pavan, I. C. B., Yokoo, S., Granato, D. C., Meneguello, L., Carnielli, C. M., Tavares, M. R., et al. (2016). Different Interactomes for P70-S6K1 and P54-S6K2 Revealed by Proteomic Analysis. *Proteomics* 162650–162666. doi: 10.1002/pmic.201500249

Perwitasari, O., Johnson, S., Yan, X., Howerth, E., Shacham, S., Landesman, Y., et al. (2014). Verdinexor, a Novel Selective Inhibitor of Nuclear Export, Reduces Influenza A Virus Replication *in Vitro* and *In Vivo*. *J. Virol.* 88, 10228–10243. doi: 10.1128/jvi.01774-14

Perwitasari, O., Johnson, S., Yan, X., Register, E., Crabtree, J., Gabbard, J., et al. (2016). Antiviral Efficacy of Verdinexor *In Vivo* in Two Animal Models of Influenza a Virus Infection. *PloS One* 11, e0167221–0167232. doi: 10.1371/journal.pone.0167221

Sanche, S., Lin, Y. T., Xu, C., Romero-Severson, E., Hengartner, N., and Ke, R. (2020). Research High Contagiousness and Rapid Spread of Severe Acute Respiratory Syndrome Coronavirus 2. *Emerg. Infect. Dis.* 26, 1470–1477. doi: 10.3201/eid2607.200282

Siddiqui, K., On, K. F., and Diffley, J. F. X. (2013). Regulating DNA Replication in Eukarya. *Cold Spring Harb. Perspect. Biol.* 5, a012930–012939. doi: 10.1101/cshperspect.a012930

Song, Y., Zhang, M., Yin, L., Wang, K., Zhou, Y., Zhou, M., et al. (2020), 106080–106086. Covid-19 Treatment: Close to a Cure? A Rapid Review of Pharmacotherapies for the Novel Coronavirus (SARS-Cov-2). *Int. J. Antimicrob. Agents* 56, 1060807–106086. doi: 10.1016/j.ijantimicag.2020.106080

Strzalka, W., and Ziemienowicz, A. (2011). Proliferating Cell Nuclear Antigen (PCNA): A Key Factor in DNA Replication and Cell Cycle Regulation. *Ann. Bot.* 107, 1127–1140. doi: 10.1093/aob/mcq243

Stukalov, A., Girault, V., Grass, V., Karayel, O., Bergant, V., Urban, C., et al. (2021). Multilevel Proteomics Reveals Host Perturbations by SARS-CoV-2 and SARS-Cov. *Nature.* 594 (7862), 246–252. doi: 10.1038/s41586-021-03493-4

Thiel, V., Ivanov, K. A., Putics, Á., Hertzig, T., Schelle, B., Bayer, S., et al. (2003). Mechanisms and Enzymes Involved in SARS Coronavirus Genome Expression. *J. Gen. Virol.* 84, 2305–2315. doi: 10.1099/vir.0.19424-0

Tsurimoto, T. (1998). PCNA, a Multifunctional Ring on DNA. *Biochim. Biophys. Acta - Gene Struct. Expr.* 1443, 23–39. doi: 10.1016/S0167-4781(98)00204-8

Warbrick, E. (1998). PCNA Binding Through a Conserved Motif. *BioEssays* 20, 195–199. doi: 10.1002/(SICI)1521–1878(199803)20:3<195::AID-BIES2>3.0.CO;2-R

WHO- World Health Organization (2020). Who. Coronavirus Disease (COVID-2019) Situation Reports.

Widman, D. G., Gornisiewicz, S., Shacham, S., and Tamir, S. (2018). *In Vitro* Toxicity and Efficacy of Verdinexor, an Exportin 1 Inhibitor, on Opportunistic Viruses Affecting Immunocompromised Individuals. *PloS One* 13, e0200043–0200053. doi: 10.1371/journal.pone.0200043

Witko-Sarsat, V., Mocek, J., Bouayad, D., Tamassia, N., Ribeil, J. A., Candalh, C., et al. (2010). Proliferating Cell Nuclear Antigen Acts as a Cytoplasmic Platform Controlling Human Neutrophil Survival. *J. Exp. Med.* 207, 2631–2645. doi: 10.1084/jem.20092241

Wu, A., Peng, Y., Huang, B., Ding, X., Wang, X., Niu, P., et al. (2020). Genome Composition and Divergence of the Novel Coronaviru-Ncov) Originating in China. *Cell Host Microbe* 27, 325–328. doi: 10.1016/j.chom.2020.02.001

Wyler, E., Mösbauer, K., Franke, V., Diag, A., Gottula, L. T., Arsie, R., et al. (2020). Bulk and Single-Cell Gene Expression Profiling of SARS-CoV-2 Infected Human Cell Lines Identifies Molecular Targets for Therapeutic Intervention. *bioRxiv*. doi: 10.1101/2020.05.05.079194

Yin, L., Xie, Y., Yin, S., Lv, X., Zhang, J., Gu, Z., et al. (2015). The S-nitrosylation Status of PCNA Localized in Cytosol Impacts the Apoptotic Pathway in a Parkinson's Disease Paradigm. *PloS One* 10, e0117546–0117550. doi: 10.1371/journal.pone.0117546

Zeman, M. K., and Cimprich, K. A. (2014). Causes and Consequences of Replication Stress. *Nat. Cell Biol.* 16, 2–9. doi: 10.1038/ncb2897

Zhang, J., Cruz-cosme, R., Zhuang, M. W., Liu, D., Liu, Y., Teng, S., et al. (2020). A Systemic and Molecular Study of Subcellular Localization of SARS-CoV-2 Proteins. *Signal Transduction Targeting Ther.* 5, 269–275. doi: 10.1038/s41392-020-00372-8

Zheng, Y., Zhuang, M. W., Han, L., Zhang, J., Nan, M. L., Zhan, P., et al. (2020). Severe Acute Respiratory Syndrome Coronavirus 2 (SARS-CoV-2) Membrane (M) Protein Inhibits Type I and III Interferon Production by Targeting RIG-I/MDA-5 Signaling. *Signal Transduction Targeting Ther.* 5, 299–306. doi: 10.1038/s41392-020-00438-7

Conflict of Interest: The authors declare that the research was conducted in the absence of any commercial or financial relationships that could be construed as a potential conflict of interest.

Publisher's Note: All claims expressed in this article are solely those of the authors and do not necessarily represent those of their affiliated organizations, or those of the publisher, the editors and the reviewers. Any product that may be evaluated in this article, or claim that may be made by its manufacturer, is not guaranteed or endorsed by the publisher.